Cryobiology 113 (2023) 104592

Contents lists available at ScienceDirect

Cryobiology

journal homepage: www.elsevier.com/locate/cryo

Identification of a fundamental cryoinjury mechanism in MSCs and its mitigation through cell-cycle synchronization prior to freezing

Brian H. Johnstone [1], Dongsheng Gu [1], Chieh-Han Lin, Jianguang Du, Erik J. Woods [*]

Ossium Health, Inc., Indianapolis, IN, United States

ARTICLE INFO

Keywords:
MSC
Serum starvation
Immune suppression
Cryopreservation
Cryogenic injury
Cellular therapy
Cell cycle
DNA replication
DNA double-stranded breaks

ABSTRACT

Clinical development of cellular therapies, including mesenchymal stem/stromal cell (MSC) treatments, has been hindered by ineffective cryopreservation methods that result in substantial loss of post-thaw cell viability and function. Proposed solutions to generate high potency MSC for clinical testing include priming cells with potent cytokines such as interferon gamma (IFNγ) prior to cryopreservation, which has been shown to enhance post-thaw function, or briefly culturing to allow recovery from cryopreservation injury prior to administering to patients. However, both solutions have disadvantages: cryorecovery increases the complexity of manufacturing and distribution logistics, while the pleiotropic effects of IFNγ may have uncharacterized and unintended consequences on MSC function. To determine specific cellular functions impacted by cryoinjury, we first evaluated cell cycle status. It was discovered that S phase MSC are exquisitely sensitive to cryoinjury, demonstrating heightened levels of delayed apoptosis post-thaw and reduced immunomodulatory function. Blocking cell cycle progression at G0/G1 by growth factor deprivation (commonly known as serum starvation) greatly reduced post-thaw dysfunction of MSC by preventing apoptosis induced by double-stranded breaks in labile replicating DNA that form during the cryopreservation and thawing processes. Viability, clonal growth and T cell suppression function were preserved at pre-cryopreservation levels and were no different than cells prior to freezing or frozen after priming with IFNγ. Thus, we have developed a robust and effective strategy to enhance post-thaw recovery of therapeutic MSC.

1. Introduction

The demonstrated potential of mesenchymal stem/stromal cells (MSC) to address intractable diseases has been slow to materialize into approved therapies. Development of the MSC field has been hindered by a lack of clear efficacy in late-stage, multi-center, randomized controlled trials, even though preclinical and early-stage trials have appeared exceptionally positive. The disconnect between promising early data and demonstrating unequivocal clinical efficacy for other than a handful of diseases has been broadly attributed to batch-to-batch variation of critical quality attributes caused by non-optimal manufacturing practices [16,17,32]. Advanced manufacturing methods and strong quality assurance systems can prevent release of nonconforming MSC lots; however, an adequate supply of primary cell stocks are necessary to economically manufacture cells without overexpansion, which induces senescence and loss of potency [22,36].

Other sources of variability are injury due to cryopreservation of intermediate cell stocks used in manufacturing and final products as well as improper handling of the cells during thawing for administration [10,17,36]. Cryopreservation is an essential process for maintaining viability during manufacturing and subsequent storage and shipment of cellular therapies. However, substantial loss of function after thawing is commonly observed and is a major hurdle impeding full realization of the broad clinical potential of all cellular therapeutics, including MSC [37]. Thus, establishing procedures that overcome cryoinjury are of paramount importance for enhancing clinical successes with MSC therapies. One presently employed solution is to briefly (commonly 18–72 h) culture MSC after thawing so that the cells have time to recover (ideally without proliferating) prior to infusion into patients [4]. Besides adding to costs for treatment by requiring personnel time and material

Abbreviations: MSC, mesenchymal stem/stromal cells; hPL, human platelet lysate; γH2AX, phosphorylated histone variant H2AX; DSB, DNA double stranded breaks; EdU, Ethylnyl-2′-deoxyuridine; IFNγ, interferon gamma; CFU-F, colony forming unit-fibroblast.

* Corresponding author.
E-mail address: erik@ossiumhealth.com (E.J. Woods).

[1] Co-first authors.

https://doi.org/10.1016/j.cryobiol.2023.104592
Received 27 April 2023; Received in revised form 4 October 2023; Accepted 9 October 2023
Available online 11 October 2023

resources, cryorecovery adds logistical complexity to the treatment given the lability of cells during shipment and the short product expiration window. Developing a procedure that enables thawing and infusing functional cells at the patient's bedside would be much more advantageous.

It has been suggested that so called "cryoinjury" and related thawing injury were major contributors to high profile failures of MSC therapies in advanced phase clinical trials [16]. In addition to the immediately observable lower viability upon thaw, cryoinjured MSC display diminished immunomodulatory activity and an increased susceptibility to clearance *in vivo* [10,15,39]. The causes of cryoinjury are multifaceted and include osmotic and thermal shock, cryoprotectant toxicity, and intracellular ice crystal formation [60]. Each of these insults can lead to a sequelae of physiological responses, further enhancing cell injury during recovery [5]. These delayed effects, which manifest over hours and days, are more accurate predictors of post-thaw cellular yield and function compared to immediate post-thaw viability assessments [5]. Thus, sampling at intervals rather than at a discrete timepoint immediately post-thaw is required; however, it is not practical to collect this data prior to administering MSC in the clinical setting.

Strategies to prevent or at least limit cellular injury during cryopreservation and thawing generally include: developing cryopreservation solutions which mirror intracellular ion species and concentrations; optimization of cooling and warming rates; novel cryoprotectant agents; inhibitors of cell injury processes; and ice recrystallization inhibitors [2]. Although promising results have been attained, it is likely that a single solution that is effective across different cell types, having vastly different physiological characteristics might not be achievable.

Even for a homogeneous population, cell expansion in nutrient-rich media generates a spectrum of physiological states due to asynchronous progression of the population through the cell cycle [20,42]. Following mitosis (M phase), cells entering the gap 1 (G1) phase of the cell cycle are relatively compact in size, expanding until reaching the DNA synthesis (S) phase at which point chromosomes decondense during replication, followed by continued growth in gap 2 (G2) prior to chromosome condensation and another mitosis event [20]. Cells that temporarily exit the cell cycle are described as resting in the gap 0 (G0) phase. Besides a gradual increase in volume which occurs as daughter cells expand and replicate DNA, mitotic phase cells rapidly swell by up to 30 % due to a rapid influx of water, resulting in reduced density and osmolality of the cytoplasm [7,52,63]. Thus, cells in different phases of the cell cycle possess different intracellular compositions and volumes. Furthermore, and in contrast to a generalized view of populations of proliferating cells, on the individual cell level, mass and volume oscillate nonparametrically in response to a multitude of extrinsic and intrinsic modulators and somewhat autonomously with respect to the stage in the cell cycle [6–8,43,54]. For instance, checkpoint regulation due to DNA strand breaks will either stop or slow cell cycle progression, depending on the phase of the cell cycle, until repairs are complete [9]. If repairs cannot be completed due to the severity of DNA damage, exit from the cell cycle will be triggered to prevent passing on damaged DNA to daughter cells.

The differences in size and internal composition of asynchronously proliferating monocultures produce a spectrum of physiological states with a commensurate range of responses to osmotic imbalances, hypothermia and phase transitions during freezing and warming. The ability of cells to tolerate the rather harsh conditions experienced during cryopreservation depends on cell size (surface-to-volume ratio), membrane permeability and osmotic constraints [60]. Cell volume is governed through an equilibrium between internal hydrostatic pressure, osmolarity, and membrane tension with each fluctuating due to active transport and passive diffusion of water, small solutes and ions across the membrane over timescales of minutes to hours [24,38]. Thus, hydrodynamic forces acting on individual cells within a population are constantly in flux, leading to a distribution of responses to sudden changes in external osmolarity that occur during addition or removal of molar concentrations of commonly used cryoprotectants such as dimethyl sulfoxide (Me_2SO). Relatedly, water content will influence the extent of ice crystal formation and the concentrations of monomeric precursors (e.g., amino acids, nucleosides and monosaccharides) versus polymeric structures influence on internal osmolality. Thus, dynamic fluctuations in cell size and composition throughout the cell cycle will influence tolerance limits to the cryopreservation and thawing processes.

Given this potential for high cell cycle variability with MSC cultures, we sought to examine the effects of cell cycle status on susceptibility of MSC to injury due to cryopreservation and subsequent thawing. In this work it was discovered that MSC in S phase are exquisitely sensitive to cryoinjury even in the presence of a cryoprotective additive, demonstrating heightened levels of apoptosis post-thaw and reduced immunomodulatory function. Synchronizing MSC cultures by growth factor deprivation (also known as serum starvation) to block progression through G1 phase prior to cryopreservation greatly reduced post-thaw dysfunction of the cells by preventing DNA double strand breaks (DSB) during replication and subsequent triggering of apoptosis. Thus, we have developed a robust and effective strategy to enhance post-thaw recovery of therapeutic MSC.

2. Materials and methods

MSC culture, synchronization by starvation and cryopreservation. Deceased donor-derived vertebral bone marrow (BM) MSC were isolated, cultured and expanded utilizing our published methods [22]. Briefly, eluted vertebral body BM obtained from 3 deceased donors was seeded in separate CellBIND T-225 flasks (Corning, MA, USA) at a density of $2.5x10^4$ viable cells/cm^2 with αMEM (Biologos, Montgomery, IL, USA) containing 10 % human platelet lysate (hPL; Stemulate®, Sexton, Indianapolis, IN, USA), 2 ng/ml each of recombinant human epidermal growth factor (rhuEGF; R&D Systems, Minneapolis, MN, USA) and recombinant human basic fibroblast growth factor (bFGF; R&D Systems) and maintained at 5 % humidified CO_2 and 37 °C. At 70 % confluence cells were detached using 1x TrypLE (Thermo Fisher Scientific, Waltham, MA, USA) and sub-cultured at a density of 4000 cells/cm^2 until passage 4 for use in experiments. Umbilical cord and adipose MSC were purchased from Lonza (Morristown, NJ, USA) and live donor BM-MSC were purchased from RoosterBio (Frederick, MD, USA). All MSC, regardless of the source, were cultured in the medium described above.

Synchronization to G0/G1 by hPL starvation: When passage 4 MSC in T175 flasks attained 70–80 % confluency, the cells were washed once with 20 ml αMEM and then cultured in αMEM or αMEM containing 0.1 % hPL for another 24–48 h. Where indicated, IFNγ (R&D Systems) was also added to the medium at a final concentration of 25 ng/ml during starvation.

To cryopreserve MSCs, cells were harvested from cultures using TrypLE, pelleted and generally resuspended in pre-chilled Me_2SO-based freezing solution (Plasma-Lyte; Baxter, Deerfield, IL, USA; containing 2.5 % human serum albumin; Octapharma, Paramas, NJ, USA; supplemented with 5 % Me_2SO; Biolife Solutions, Bothell, WA, USA) at a density of 1×10^6 cells/ml and aliquoted into cryovials. Vials were placed in a CoolCell (Corning Life Sciences, Durham, NC, USA) and frozen in a −80 °C freezer overnight before storage in liquid nitrogen vapor.

In some experiments either glycerol or propylene glycol (both purchased from Sigma, MO USA) was used as alternative cryoprotective agents (CPAs). These solutions contained 2.5 % HSA supplemented with 5 % glycerol or propylene glycol (PG) in Plasma-Lyte. To test the CPA effect on cells without cryopreservation, P4 MSCs were harvested and resuspended in freezing solutions made of Me_2SO, glycerol or PG at a density of 1×10^6 cells/ml and incubated at room temperature for 1 h. The cells suspended in CPA-free solution were used as controls for pre-cryopreservation analysis. A portion of the cells in each solution was

also frozen as described above.

For thawing, all vials were removed from liquid nitrogen and quickly placed in a 37 °C water bath until a small amount of ice remained. Cells were then gently transferred into 15 ml conical tubes containing 10 ml pre-warmed media, centrifuged at 500×*g* for 5 min, and resuspended in 1 ml pre-warmed media for use in downstream applications.

For the colony forming unit-fibroblast (CFU–F) assay, 100 viable continuously cultured or thawed MSC were plated in triplicate wells of 6-well plates in MethoCult™ medium (StemCell Technologies, Vancouver, BC Canada). The plates were placed in a humidified incubator in an atmosphere of 5 % CO_2 and maintained at 37 °C. After 11 days, the cultures were washed with PBS and fixed with methanol, followed by 0.5 % crystal violet staining. A cell cluster that had more than 50 cells was counted as a colony under microscopy.

Apoptosis assay. Post-thaw apoptosis of MSC was assessed by staining the cells at different time points with annexin V-APC (Biolegend, San Diego, CA, USA) and DAPI (Biolegend). Briefly, thawed cells were plated in 6-well plates at $2x10^5$ per well and allowed to recover by being placed in a 37 °C incubator. Cells immediately after thawing served as the 0 h time point. At various time points (2, 4, 6, and 8 h), cells (both floating and attached) were harvested and stained with annexin V-APC and DAPI (0.5ug/ml) in annexin V binding buffer (Thermo Fisher Scientific) according to manufacturer's instruction. A NovoCyte flow cytometer (Agilent Technologies, Santa Clara, CA, USA) was used for data collection, and data were analyzed using NovoExpress software (Agilent). To determine DNA content in apoptotic population, annexin V-stained MSC were fixed with 3.7 % formaldehyde solution by diluting the 37 % formaldehyde stock (Sigma-Aldrich, Saint Louis, MO, USA) and followed by permeabilization with 0.5 % Triton X-100. Then cells were treated with 10 μg/ml RNase (Sigma-Aldrich) to remove RNA and subsequently stained with propidium iodide (Biotium, Fremont, CA, USA) and analyzed by flow cytometry. Annexin V binding buffer was used for the entire procedure to enhance binding of annexin V-APC on the surface of the cells.

Ethylnyl-2′-deoxyuridine (EdU) incorporation assay. To determine the DNA incorporation efficiency of S phase cells during post-thaw recovery, the EdU incorporation assay was performed using the Click-iT Plus EdU Alexa Fluor 647 Flow Cytometry Assay Kit (Thermo Fisher Scientific), according to the manufacturer's instructions. Briefly, 1 h prior to each indicated time point, 10 μM final concentration of EdU was added to each well containing post-thaw MSCs. After 1 h incubation, cells were fixed, permeabilized and the incorporated EdU was detected using Alexa Fluor 647 azide. After washing, cells were incubated in PBS containing 10 μg/ml RNase for 1 h at room temperature and subsequently stained with propidium iodide and analyzed by flow cytometry.

Detection of DNA DSB by γH2AX staining. γ-H2AX detection was performed as described by Muslimovic et al. [41]. Briefly, at indicated time points, at least 10^5 cells in 50 μl (PBS, 1 % BSA) were added to 150 μl anti-H2AXS139ph-FITC conjugate (0.6 μg/ml, EMD Millipore, Burlington, MA, USA) supplemented Block-9 staining buffer (PBS, 1 g/l BSA, 8 % mouse serum, 0.1 g/l RNaseA, 0.25 g/l herring sperm DNA, 0.1 % Triton X-100, 5 mM EDTA, and phosphatase inhibitors including 10 mM NaF, 1 mM Na_2MoO_4 and 1 mM $NaVO_3$). Staining was performed on ice in the dark for 3 h. Cell cycle distribution was monitored by adding 5 μM Vybrant dye cycle violet stain (Thermo Fisher Scientific) during the last hour of staining. The cells were then subjected to flow analysis. MSC treated with 100 μM Etoposide (Sigma-Aldrich) for 30 min were used as positive control.

Immunofluorescence microscopy. Continuously cultured or post-thawed MSC were seeded into 6-well plates at a density of $2x10^5$ per well and incubated for 2 h in the presence of 10 μM EdU in a 37 °C incubator. Cells, both floating and attached, were then collected and resuspended in PBS at 5 $x10^5$/ml and the cell suspension (75 μl/spot) was spun onto slides using a cyto-centrifuge (5 min at 1100 rpm, Cytofuge 2, Statspin, Norwood, MA, USA). The cells were then fixed with 3.7 % formaldehyde for 15 min at room temperature. After being washed with PBS, cells were permeabilized by cold methanol at −20 °C for 10 min. Next incorporated EdU was detected using the Click-&-Go® EdU 594 Cell Proliferation Assay Kit (Click Chemistry Tools, Scottsdale AZ, USA) according to manufacturer's instruction. Cells were then blocked using 5 % FBS in PBS for 1 h at room temperature followed by the addition and incubation of the following primary antibodies overnight at 4 °C: mouse anti-phospho-Histone H2A.X (Ser139) antibody (1:300, Millipore), rabbit anti- Cleaved Caspase-3 (Asp175) (1:400, Cell Signaling Technology, Danvers, MA, USA). After three washes with 0.5 % Tween in PBS, bound antibodies were detected with FITC-conjugated goat anti-mouse IgG (1:300), FITC-conjugated goat anti-rabbit IgG (1:300), and DyLight 594 conjugated goat anti-rabbit IgG (1:300) at room temperature for 2 h. All secondary antibodies were purchased from Boster Biological Technology (Pleasanton, CA, USA). After three washes, 5 μg/ml Hoechst 33342 PBS solution was used for DNA stain and fluorescent images were obtained by Leica DM4B system (Leica, Wetzlar, Germany).

T cell suppression assay. Fresh whole blood was purchased from Versiti Blood Center (Indianapolis, IN, USA). Peripheral blood mononuclear cells (PBMCs) were isolated using Ficoll-Paque® (Cytiva, Marlborough, MA, USA) density gradient centrifugation. The isolated PBMCs were labeled with carboxyfluorescein succinimidyl ester (CFSE; BD Bioscience) at a concentration of 5 μM per $20x10^6$ cells at room temperature for 10 min, followed by cryopreservation in 90 % FBS/10 % Me_2SO. Thawed MSC were seeded in RPMI with 10 % FBS at a density of 1.2×10^5 or 2.4×10^5 cells per well of a 24-well plate and cultured for 24 h. The supernatants were carefully removed and 1.2×10^6 CFSE-labeled PBMCs in RPMI with 10 % FBS were added into each well. The PBMCs were activated using αCD3ε antibody (Bio X Cell, Lebanon, NH, USA) at a concentration of 150 ng/ml. The MSC were co-cultured with the PBMCs at 37 °C for 4 days. Cell proliferation was determined by monitoring CFSE dilution in $CD4^+$ and $CD8^+$ T cells by flow cytometry. Proliferation of T cells is reported as the replication index which was calculated by dividing the sum of the percentage of all populations derived from the original parental population by the percentage of the original parental population.

Statistical analyses. Results are expressed as the mean ± SD. All statistical comparisons were made using Prism 9 (GraphPad Software Inc, La Jolla, CA, USA). Statistical tests used to analyze each data set are indicated in the figure legends. A *t*-test was used to compare two data sets. One-way ANOVA with Tukey's multiple comparisons test or Two-way ANOVA with Šídák's multiple comparisons tests were performed when more than two data sets were compared. Differences with p-values <0.05 were considered significant.

3. Results

Apoptosis of freshly cultured (i.e., non-cryopreserved) and thawed cryopreserved MSC was determined by annexin V and DAPI staining (Fig. 1A). Immediately after thawing there was no difference in apoptosis and viability of cryopreserved cells compared to fresh cells (Fig. 1B and C; $P > 0.05$). The percentage of annexin V^+/$DAPI^-$ apoptotic and $DAPI^+$ dead cells increased over time in culture, peaking by approximately 4 h at 9.5 ± 0.48 % (mean ± standard deviation) and 10.0 ± 3.8 %, respectively, which were both significantly higher than immediately post-thaw ($P < 0.05$). By 4 h viable cells decreased to 81 ± 3.3 % from an initial viability of 94 ± 0.12 % (Fig. 1D). Additionally, the frequency of colony forming unit-fibroblast cells (CFU–F), which is an indication of clonogenicity, was severely compromised in cryopreserved MSC (Fig. 1E). Thus, immediate post-thaw analysis is not a reliable predictor of cell health, which decreases substantially over time even when cells are cultured in optimized nutrient-rich conditions.

Delayed apoptosis and death were confined to a small percentage of thawed cells, suggesting that catastrophic cryoinjuries, such as Me_2SO-induced toxicity and osmotic stress, were not the primary causes of progressive viability loss after 2 h in culture. This was confirmed by

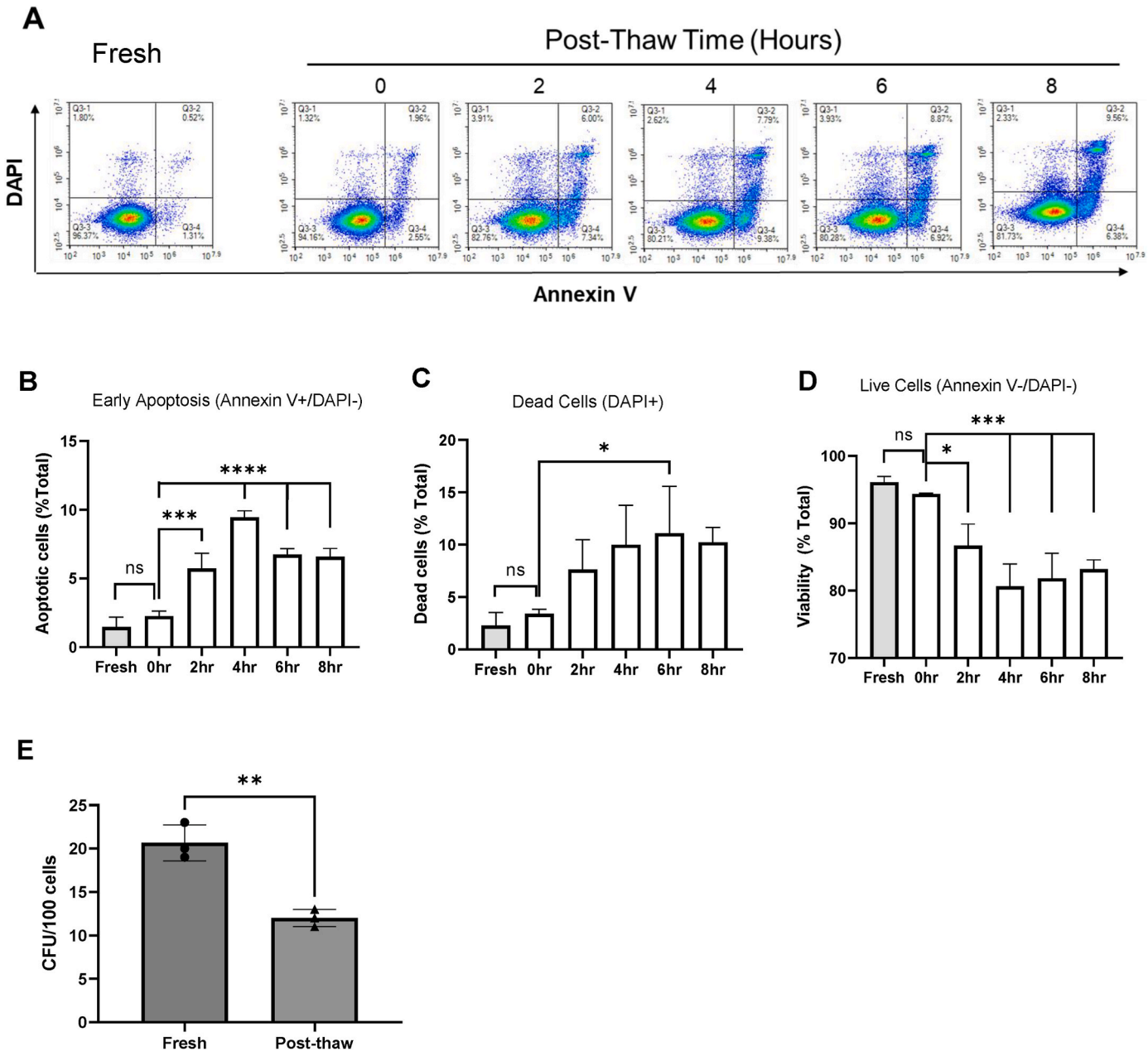

Fig. 1. Cryopreservation of MSCs induces cell death during post-thaw recovery in culture. (**A**) Representative flow cytometry plots showing early apoptosis (lower right quadrant and death (upper quadrants) of post-thaw MSCs compared to cells prior to cryopreservation ("fresh"). Quantitation of post-thaw (**B**) apoptotic, (**C**) dead and (**D**) live cells at the times indicated after thawing and culturing compared to freshly cultured cells. (**E**) Colony forming unit-fibroblast (CFU–F) counts after 11 days of culturing MSC prior to (fresh) and after (post-thaw) cryopreservation. Data are displayed as mean ± SD from 3 independent experiments using a single donor MSC, which are representative of data obtained using MSC from the two other donors. (**F**) Asterisks indicate statistical significance of the indicated comparisons: *, $p < 0.05$; **, $p < 0.01$; ***, $p < 0.001$, ****, $p < 0.0001$. Non-significance (ns) is only indicated for comparisons of fresh versus immediately post-thaw cells but is implied if comparisons did not achieve significance ($p < 0.05$). Fresh and 0 h post-thaw data as well as CFU data compared by unpaired *t*-test. Post-thaw recovery timepoints (B–D) compared by one-way ANOVA with Šídák's multiple comparisons test.

evaluating apoptosis levels after extended incubation at room temperature in PBS, Me_2SO, glycerol or PG prior to freezing (Fig. S1A). A progressive increase in DNA DSB was observed after thawing MSC cryopreserved in the three different CPAs tested. (Fig. 1E and S1B). The percentage of cells with DSB was higher ($P < 0.001$) in cells cryopreserved in 5 % Me_2SO (4.1 ± 0.2 %, mean ± SD) than in either 5 % glycerol (1.7 ± 0.3 %) or 5 % PG (2.4 ± 0.1 %).

It was recently reported that cryopreservation induces breaks in single-stranded DNA during S phase replication [13]. It was demonstrated that single-stranded lesions were initially formed, followed by DSB and disruptions of chromatin higher order. Thus, we investigated apoptosis in relation to cell cycle status and correlated this to DNA synthesis (Fig. 2). Compared to continuously culturing or post-thaw recovery for 24 h, the fluorescence intensity of EdU staining was reduced, indicating compromised DNA synthesis in thawed MSC (Fig. 2A). This decline suggested that S phase cells were impacted by freezing and thawing. Analysis of apoptosis indicated that S phase cells were disproportionately represented in the population of dying cells (32.4 ± 4.6 %) compared to the annexin V^- population (12.9 ± 1.9 %) of S phase cells, indicating that MSC in this phase were more labile to cryoinjury (Fig. 2B and C).

The presence of DNA DSB in thawed MSC was detected by labeling

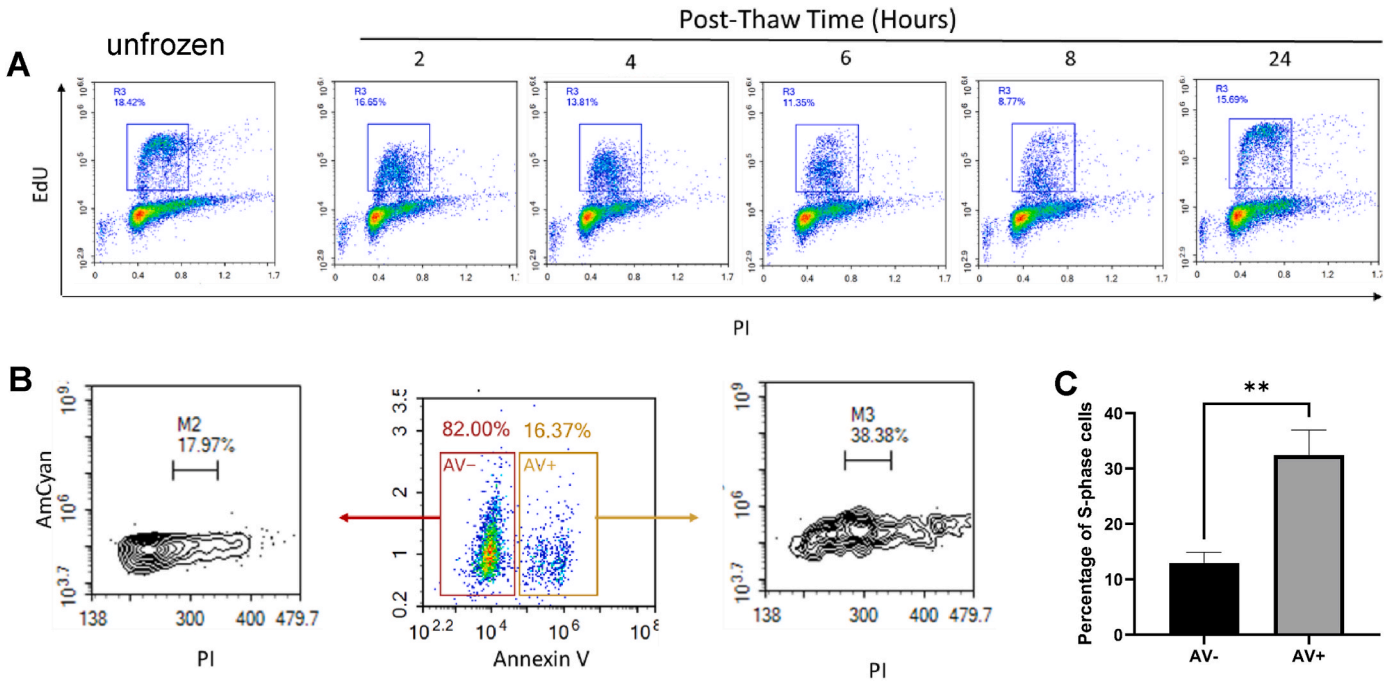

Fig. 2. Replicating S phase MSCs demonstrated reduced DNA synthesis and higher levels of apoptosis after cryopreservation and subsequent thawing. (**A**) Flow plots showing EdU incorporation efficiency in S-phase MSCs during post-thaw recovery. (**B**) Representative gating strategy for enumerating S phase cells in annexin V- (AV-) and annexin V+ (AV+) populations at 4 h post-thaw. Gates and percentages shown on contour plots represent cells in S phase. (**C**) Quantitation of the percentage of S phase cells in the total AV- and AV + populations obtained from 4 independent experiments. All data are presented as means ± SD. **, $p < 0.01$; paired, two-tailed *t*-test.

with an antibody to H2AX subunits surrounding the breaks which are phosphorylated (termed γH2AX) within minutes of DNA damage (Fig. 3) [29,48]. It was first confirmed that γH2AX could be measured in the assay conditions employed in this study, using the topoisomerase II inhibitor etoposide as a positive control which induced extensive DSB (Fig. 3A). Cryopreserved MSC from multiple donors were then evaluated for DSB at increasing time intervals after thawing. Very few γH2AX$^+$ cells were detected immediately after thawing (Fig. 3B and C). Double-stranded breaks were observed at 1 h post-thaw in MSC from 3 donor sources, with a peak in frequency of γH2AX$^+$ MSC at 3 h (Fig. 3D). The frequency of cells harboring DSB declined between 3 and 4 h post-thaw, which correlates with a peak in apoptosis at 4 h, suggesting that this population progressively loses viability as a result of DNA damage (Fig. 1B).

The association between increased apoptosis and S phase cells harboring DSB led to an examination of whether blocking progression to the DNA replication phase, and thereby preventing formation of labile single-stranded DNA, would protect cryopreserved cells. Serum starvation to deprive cells of mitogenic growth factors is a well-established method for synchronizing cells through inducing quiescence at G0, thus, blocking entry to S phase [10,15,39,44,46,56]. Preliminary experiments were performed to determine appropriate levels of "serum starvation," in this case deprivation of human platelet lysate (hPL). Cells were transferred from nutrient-rich medium containing 10 % hPL to base medium either totally devoid of hPL or containing a very low level (0.1 %) of hPL and cultured for 24 and 48 h. The cell morphology was unchanged by starvation; however, there was a diminution in size (Figs. S2A and B). The percentage of cells undergoing apoptosis for both starvation conditions was similar to non-starved cells at 24 h (Figs. S2C and D). Conversely, MSC were adversely impacted by hPL starvation for longer periods as indicated by a more than doubling of the percentage of apoptotic cells at 48 h, which was reflected in lower cell counts at this time (Fig. S2E). DNA synthesis was barely detectable by 24 h, indicating that the MSC exited the cell cycle during the starvation period (Fig. S2F).

The impact of starvation on classical properties of MSC was next examined. Starving the cells did not alter expression of surface markers commonly associated with MSC (Fig. S3A). Additionally, starved MSC cultured in complete growth medium were responsive to interferon-γ (IFNγ) priming, as evidenced by increased surface expression of Class II human leukocyte antigen (HLA) DR and programmed death ligand 1 (PD-L1) (Fig. S3B). Interestingly, gene expression of the immunoregulatory protein, indoleamine 2,3-dioxygenase-1 (IDO-1), increased with starvation (Fig. S3C). There was also a slight additive increase in IDO-1 protein expression with the combination of starvation and IFNγ priming (Fig. S3D). These preliminary experiments indicated that culturing MSC for 24 h under conditions of hPL deprivation was sufficient to block progression to S phase and didn't promote any obvious deleterious effects. Furthermore, starvation of MSC did not fundamentally alter the phenotype or responses to environmental stimuli.

To determine the impact of growth factor starvation on post-thaw recovery of MSCs, cells were transferred from complete medium to basal medium without hPL and cultured for 24 h. The majority of cells were in G0/G1 as indicated by the absence of DNA synthesis (Fig. 4A). Apoptosis of both starved and non-starved MSC was analyzed prior to cryopreservation and following thawing and culturing in complete medium for 4 and 8 h. Starving cells prior to cryopreservation greatly reduced the number of apoptotic cells (annexin V$^+$/DAPI$^-$) after thawing (Fig. 4B and C). Furthermore, protection against cryoinjury was observed in MSC obtained from living donor iliac crest BM as well as umbilical cord and adipose tissue (Fig. 4D). This effect was observed at all timepoints measured (0–8 h). Whereas the percentage of apoptotic non-starved cells increased until 4 h, apoptosis in starved cells remained low throughout the experimental period. Similarly, the percentage of dead (DAPI$^+$) cells increased with time in culture for non-starved cells (Fig. 4D). The percentage of dead cells in starved MSC held steady during the 8 h and were significantly lower than non-starved cells at 8 h.

Importantly, starvation completely prevented the occurrence of DSB breaks in thawed cells by blocking DNA synthesis prior to cryopreserving MSC (Fig. 4E). In contrast to cells that were not starved prior to cryopreservation (Fig. 3), the percentage of γH2AX-positive cells did not

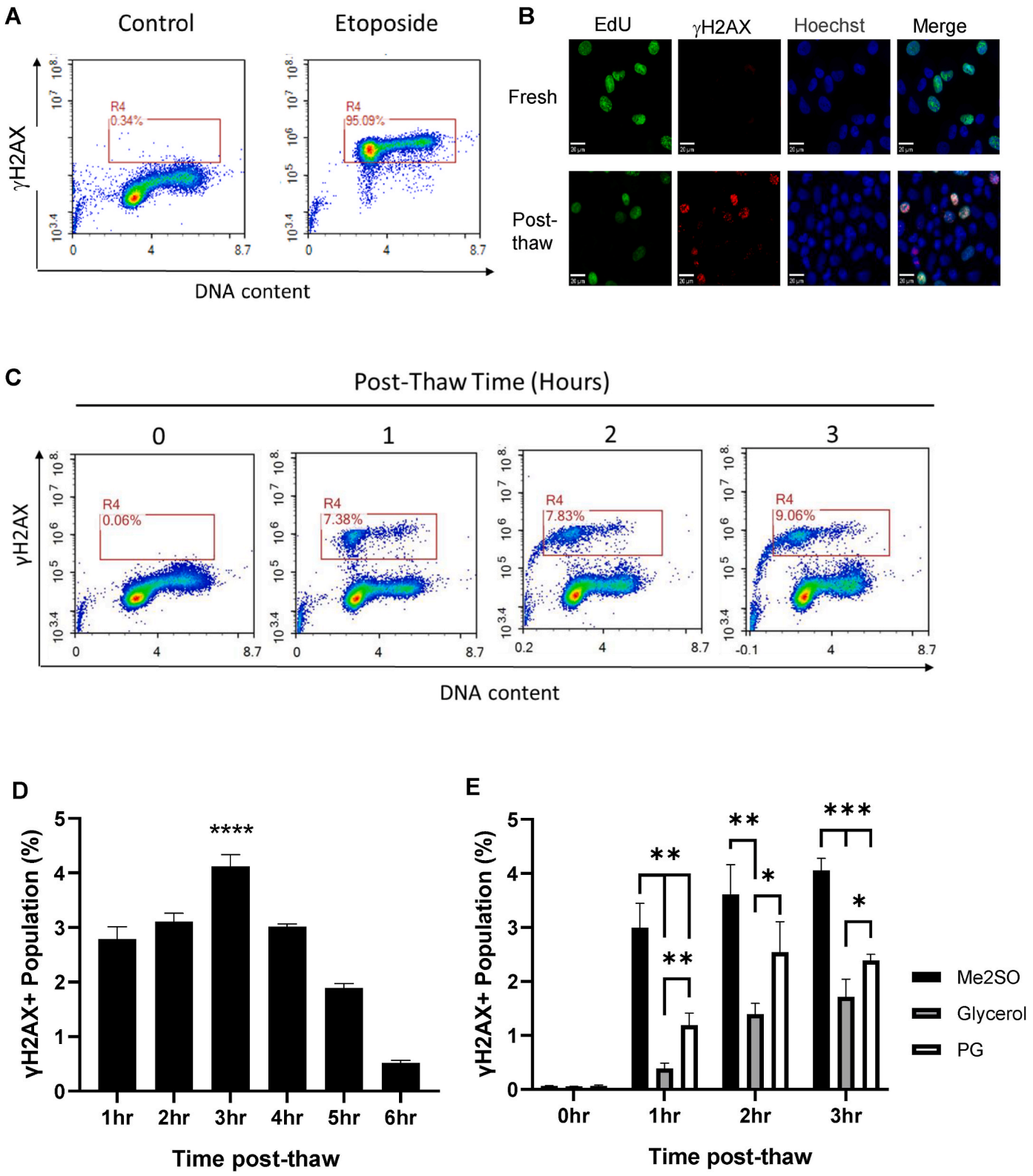

Fig. 3. Freezing and thawing induces DNA double-stranded breaks in replicating MSCs. (**A**) Flow cytometry scatter plots of γH2AX positive MSCs at baseline (control) and following etoposide (100 μM) treatment. (**B**) Immunofluorescent images of fresh and post-thaw MSC stained with EdU (green), γH2AX (red) and Hoechst 33342 nuclear stain (blue), shown individually and merged as indicated. The scale bar is 20 μm. (**C**) Representative scatter plots of γH2AX + cells at the indicated timepoints after thawing cryopreserved MSCs. (**D**) Quantitation of γH2AX + cells over time in thawed MSCs isolated from 3 independent deceased organ donors (mean ± SD). ****, $P < 0.0001$ compared to all other timepoints; one-way ANOVA with Dunnett's multiple comparisons test. (**E**) Comparison of post-thaw γH2AX + MSC when cryopreserved in either 5 % dimethyl sulfoxide (Me_2SO), 10 % glycerol or 5 % propylene glycol (PG). *, $P < 0.05$ **, $P < 0.01$; ***, $P < 0.001$; two-way ANOVA with Tukey's multiple comparisons test. (For interpretation of the references to colour in this figure legend, the reader is referred to the Web version of this article.)

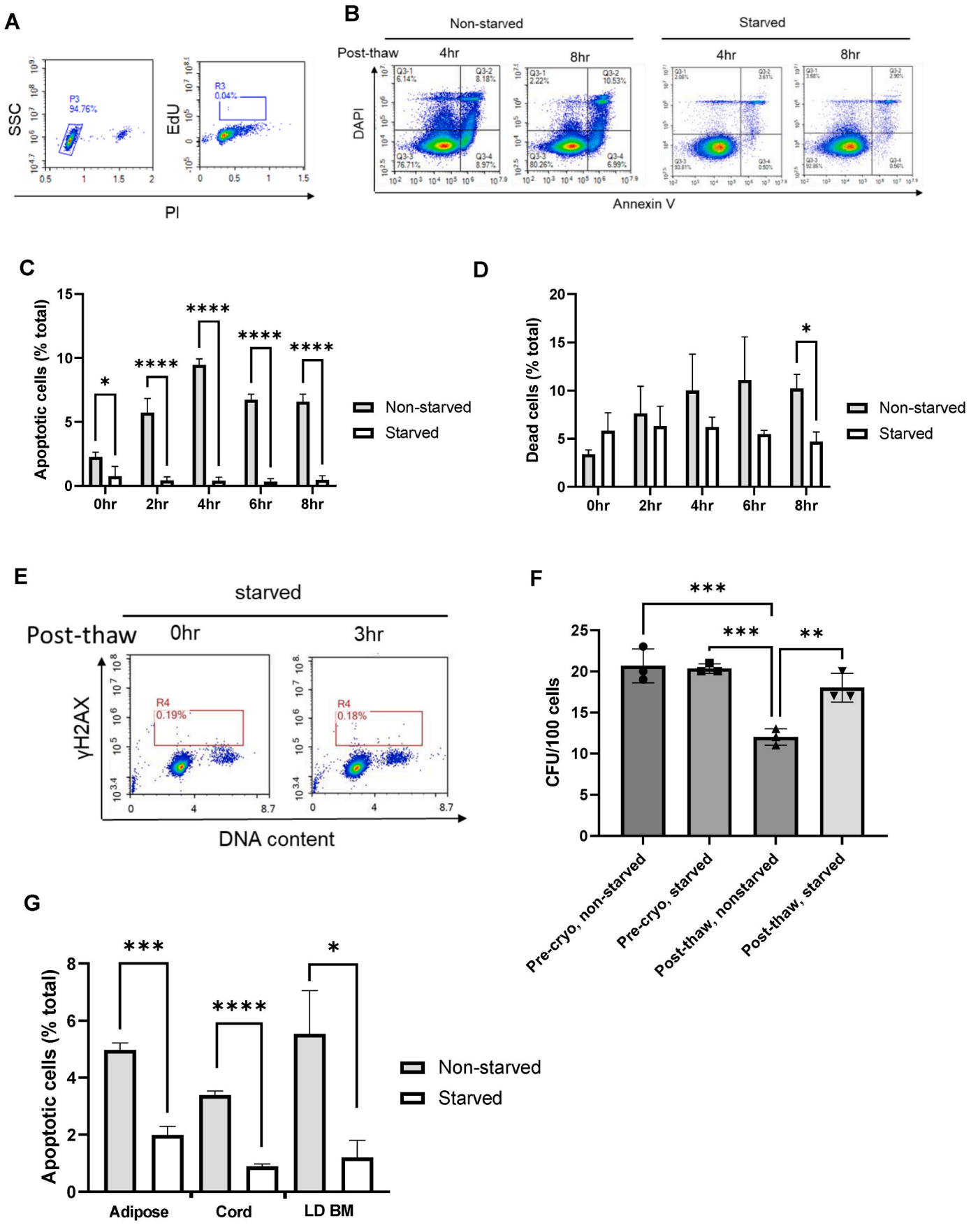

(caption on next page)

Fig. 4. Growth factor withdrawal to induce G0/G1 arrest prior to cryopreservation prevents post-thaw delayed apoptosis and death due to DNA double stranded breaks (DSB). (**A**) Cell cycle arrest prior to S phase was confirmed staining for EdU incorporation, which demonstrated that DNA synthesis was absent. (**B**) Representative flow cytometry scatter plots comparing delayed apoptosis and death in thawed MSCs that were either cultured in complete medium (non-starved) or minimal medium without hPL (starved) prior to cryopreservation. (**C**) Quantitation of apoptosis at the indicated timepoints post-thaw (mean ± SD). (**D**) Quantitation of cell death at the indicated timepoints post-thaw (mean ± SD). (**E**) Quantitation of DSB by γH2AX staining of starved MSCs following cryopreservation (compare to Fig. 3C). (**F**) CFU-F analysis of starved and non-starved MSC prior to or following cryopreservation. (**G**) Quantitation of annexin V^+ cells after thawing cryopreserved umbilical cord, adipose and iliac crest live donor (LD) BM-derived MSC. Mean ± SD for 3 independent experiments using 1–3 donors for each MSC source. *, $p < 0.05$; **, $p < 0.01$, ***, $p < 0.001$; ****, $p < 0.0001$. Two-way ANOVA with Šídák's multiple comparisons test (C and D) and one-way ANOVA with Tukey's multiple comparisons test.

increase over background levels after thawing (Fig. 4E). This phenomenon was shown to be associated with the process of cryopreservation and thawing and not caused by Me_2SO as DSB were not detected prior to cryopreservation after incubating cells for 1 h in Me_2SO or the alternative cryoprotectant agents, propylene glycol and glycerol (Fig. S1). The protective effect of growth factor starvation on cryopreserved MSC was also observed with MSC obtained from living donor iliac crest BM and MSC derived from other tissues (umbilical cord and adipose) (Fig. 4G and S4).

The impact of growth factor deprivation on the CFU-F potential of cryopreserved MSC was determined. Cells grown in complete medium prior to cryopreservation exhibited impaired ($P < 0.01$, unpaired T test) CFU-F potential compared to G0-arrested MSC (Fig. 4F). Conversely, blocking mitogenesis prior to cryopreservation resulted in CFU-F potentials that were indistinguishable from non-cryopreserved MSC.

In total, these data are highly supportive of DNA double-stranded breakage being a major factor contributing to post-thaw loss of MSC viability and function and blocking S phase entry prior to cryopreservation prevents these occurrences.

The effect of growth arrest on MSC function was further evaluated. Cryopreserved MSC have been reported by many groups to be impaired for immunosuppressive function post-thaw [10,15,39]; therefore, starved and non-starved cells were tested prior to cryopreservation or after thawing in T cell suppression assays. Non-starved cells demonstrated the least suppression immediately post-thaw; whereas, there was no difference in the $CD4^+$ and $CD8^+$ T cell suppressive activity between the other groups at the highest concentrations of MSC (Fig. 5 and Fig. S5). At the lowest ratio of 1:80 MSC:T cells, which comprised approximately 50 % of PBMC, post-thaw, starved MSC were significantly ($p < 0.05$) more suppressive than non-starved, freshly cultured MSC (Fig. 5B). The ratio of thawed MSC required to suppress activated T cell proliferation by 50 % (IC_{50}) was 8-fold less (1:80) without starvation than with starvation (1:10) (Fig. 5C). The IC_{50} for post-thaw starved MSC was no different than MSC prior to cryopreservation. These data suggest that growth-arrested MSC retain pre-cryopreservation levels of immunosuppressive function.

It was previously demonstrated that priming BM-MSC with IFNγ prior to cryopreservation partially rescued post-thaw viability and function [10]. Therefore, we evaluated whether IFNγ-licensing could further enhance growth-arrested MSC function post-thaw. Both starvation alone and starvation with IFNγ priming significantly ($p < 0.001$) enhanced post-thaw T cell suppression activity compared to MSC cryopreserved directly after culturing in complete medium (Fig. 6). Simultaneously starving and priming MSC enhanced T cell suppression activity over priming alone ($p < 0.05$ and $p < 0.001$, $CD4^+$ and $CD8^+$ T cells, respectively).

4. Discussion

We have developed a method for enhancing recovery of cryopreserved MSC to yield more viable and functional cells compared to traditional cryopreservation methods through cell cycle synchronization prior to cryopreservation. Observations that cell survival following cryopreservation may be impacted by the stage of cell cycle prior to freezing have been previously noted. An early report investigating cryoprotected and unprotected Chinese hamster lung fibroblasts however indicated any differential effect of cell cycle was mitigated through the use of glycerol [34]. A follow up study further investigated the same model with the addition of Me_2SO and confirmed that any cell cycle sensitivity to cryopreservation, for this cell type, was mitigated through cryoprotectant additives [35]. More recent studies investigating human T cells arrested in G0/G1 with Ribocilib prior to cryopreservation indicated that cell cycle did not play an important role impacting cryopreservation outcomes [1]. Cell cycle sensitivity to cryopreservation has also been investigated as a potential means to preferentially destroy cancer cells through cryoablation [50]. In this context, experiments were performed to determine if synchronizing a prostate cancer cell line in S phase using thymidine might allow for preferential cell destruction through freezing. While the authors did note that S-phase synchronized samples appeared to be more susceptible to injury (without any cryoprotective additive), cell cycle phase was not determined to be a critical factor in sensitivity to cell death following freezing. Based on these previous reports in the literature, it was therefore surprising to see the dramatic effect cell cycle stage had on MSC cryopreservation outcomes even with the inclusion of a cryoprotective additive.

Subjecting MSC to mitogenic factor deprivation for 24 h prior to cryopreservation induces synchronization of the entire cell population by forcing exit from the cell cycle at early G1 phase, thus, preventing entry into S phase which avoids formation of stalled single-stranded DNA replication forks that are susceptible to freeze/thaw damage [13]. It was demonstrated that freeze/thaw-induced DSB (Fig. 3) strongly contributed to programmed cell death (Fig. 1), predominantly in the S phase population (Fig. 2), during the initial culture period following thawing and culturing cryopreserved MSC. This early post-thaw injury contributed to the delayed effects of reduced viability and function observed with culture (Fig.. 2C and 5). It is important to emphasize that cell death due to cryopreservation-induced DSB is a delayed effect which only manifests with extended periods of culture *in vitro*, which presumably models kinetics of cell persistence *in vivo*. Thus, viability assessments that rely on a single timepoint at an interval close to the time of thawing cells for infusion would not be indicative of the actual physiological status of cells used for therapeutic applications. Previous reports have firmly established the functional impairment of cryopreserved MSC [10,15,39]. The present report extends these studies by providing a mechanistic explanation, which directly led to the practical solutions developed here for overcoming this serious impediment to clinical translation of MSC therapies. Furthermore, growth factor starvation can be combined with other strategies to further enhance post-thaw viability and function. For instance, we have demonstrated that combining starvation with IFNγ priming (also known as IFNγ licensing) has an additive effect on functional recovery of cryopreserved MSC (Fig. 6).

It is interesting to note that the enhanced survival afforded by preventing 15–20 % cells in a non-synchronized culture from entering S phase (Fig. 2) leads to a 4-fold enhancement in T cell suppression activity (Fig. 5). This observation indicates that synchronizing MSC to G0/G1 phase prior to cryopreservation has additional benefits in addition to enhancing post-thaw survival. A slight increase in IDO-1 mRNA and protein steady-state levels was observed in growth factor-starved cells (Fig. S3). The increase is likely insufficient to explain the full effect of starvation on enhanced T cell suppression; however, it might indicate

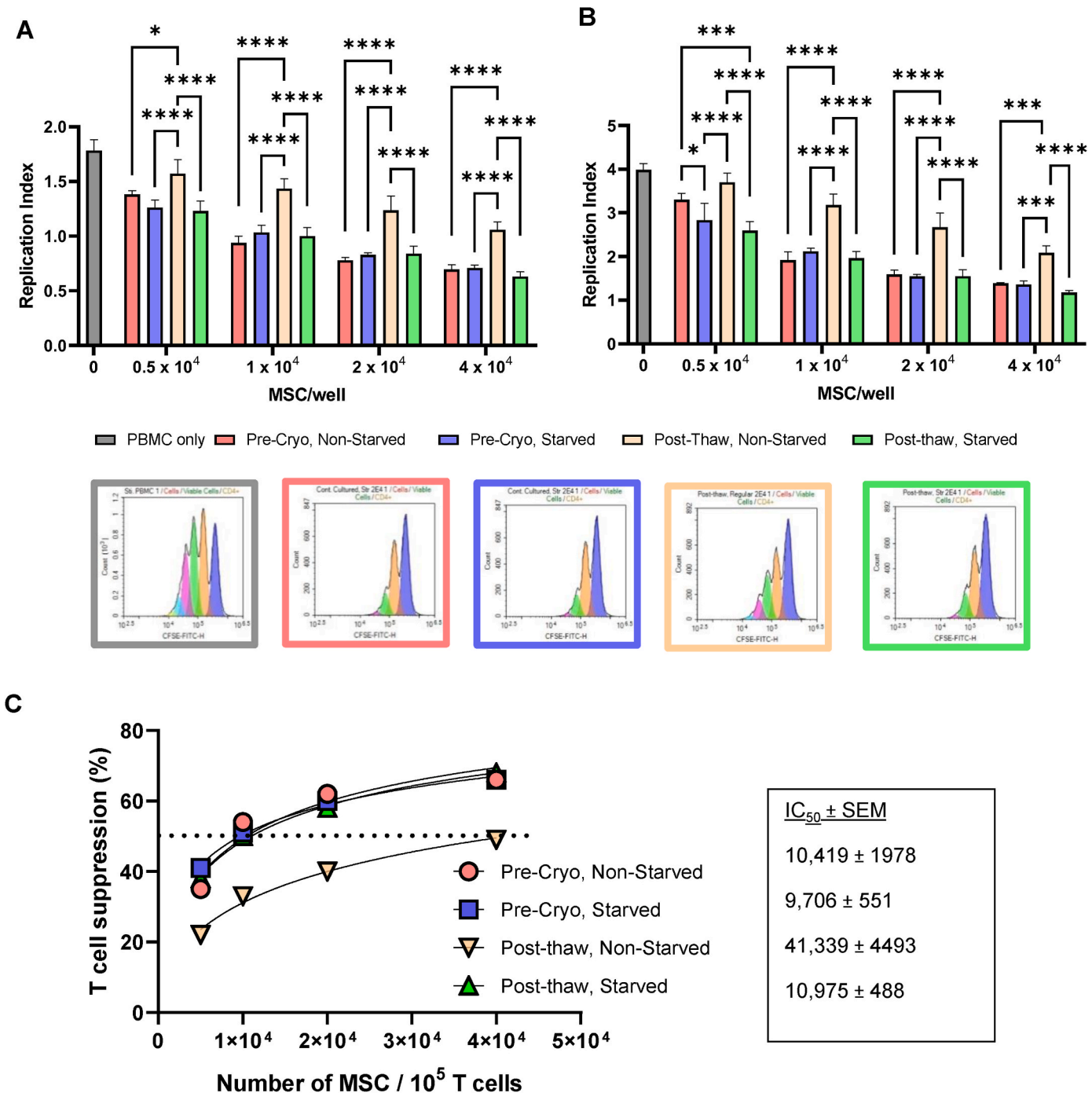

Fig. 5. The T cell suppression function of MSCs is greatly diminished by cryopreservation but can be rescued by growth factor starving the cells prior to freezing. After thawing, $2x10^4$ cells were added to wells of 96 well plates and incubated for 24 h. The medium was removed and $4x10^5$ CSFE-labeled PBMCs were added to each well. PBMCs were stimulated by adding CD3ε antibody and the plate was incubated for 4 days before analyzing T cell proliferation by flow cytometry. Proliferation of (A) $CD4^+$ and (B) $CD8^+$ T cells with different ratios of MSC to T cells which comprised 50 % of the PBMCs. The ratio of MSCs to T cells was as follows: $0.5x10^4$, 1:80; $1x10^4$, 1:40; $2x10^4$, 1:20; $4x10^4$, 1:10. Representative flow cytometry plots are shown below the bar graphs and in Fig S5 (C) The mean values for each condition tested were normalized to the maximum proliferation value obtained from the stimulated PBMC control. IC_{50} is the number of MSC that suppress 50 % of activated T cell proliferation. *, $p < 0.05$; **, $p < 0.01$; ***, $p < 0.001$; ****, $p < 0.0001$. Two-way ANOVA with Šídák's multiple comparisons test.

that growth factor deprivation confers a metabolic state that is receptive to inflammatory factor-mediated stimulation of MSC suppression. Growth factor deprivation may also enhance expression of other immunomodulatory factors. Culturing MSC under conditions that induce metabolic reprogramming has been shown to enhance anti-inflammatory cytokine expression [11,23,26,33,59,62]. It is also possible that starvation induces a quiescent state [58], which promotes greatly reduced metabolic activity, with many cell types transitioning from oxidative phosphorylation to glycolysis or fatty acid oxidation to meet basal metabolic needs [21,27,30,40,53,61]. A transition to glycolysis in response to inflammatory stimulus enhances the immunosuppressive phenotype of MSC, which may explain the results obtained here [28,55].

Prolonged growth factor starvation induces reversible exit from the

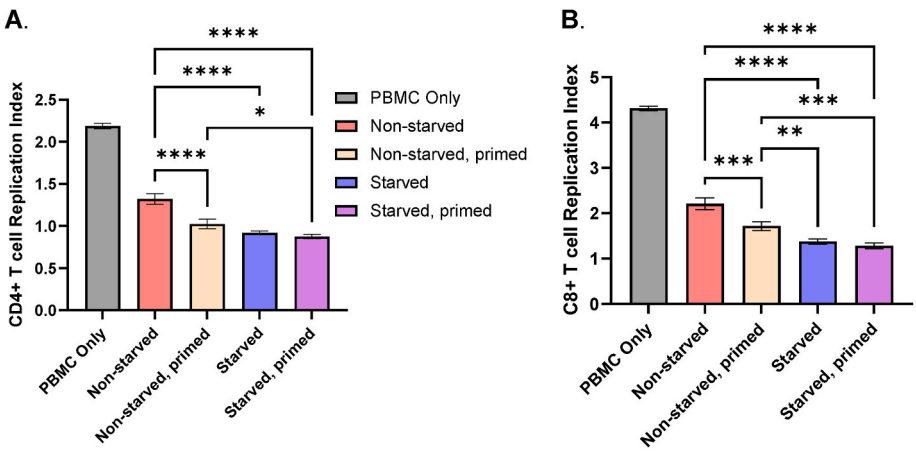

Fig. 6. Priming with IFNγ prior to cryopreservation further enhances post-thaw *in vitro* T cell suppression activity of growth factor starved MSC. Both starved and non-starved MSC were cryopreserved with and without additionally treating with IFNγ (25 ng/ml) for 24 h. Cocultures of MSC ($2x10^4$/well) and PBMC ($4x10^5$/well) were as described in the Materials & methods and legend to Fig. 5 (A) $CD4^+$ T cells. (B) $CD8^+$ T cells. *, $p < 0.05$; **, $p < 0.01$; ***, $p < 0.001$; ****, $p < 0001$. One-way ANOVA with Tukey's multiple comparisons test.

cell cycle and adoption of a quiescent state until growth conditions are favorable, at which time the cell will re-enter the cycle [58]. Quiescence is a property of stem cells as well as many lineage-restricted and differentiated cell types and is associated with increased resistance to stresses and injury as well as epigenetic changes that maintain a state of readiness for quickly responding to changes in environmental states [57]. Starvation-induced quiescence of MSC produces cells that are better able than actively proliferating cells to withstand heat shock through faster DNA repair, more rapid resumption of proliferation and preventing triggering of the senescence response [3]. Quiescent cells can exist in a primed state which was first described in skeletal satellite cells, skeletal muscle resident MSC and hematopoietic stem cells and termed G_{ALERT} [47]. Cells in the G_{ALERT} state are characterized by increased transcriptional and metabolic activity compared to quiescent (i.e., classical G0) cells and, thereby, poised to respond quickly to paracrine signals. This state has been described as "idling" [57]. It is possible that starved MSC adopt a state that promotes accelerated re-entry into the cell cycle combined with a heightened response to inflammatory signals when transferred to growth-permissive conditions.

Another probable benefit of growth factor starvation prior to cryopreservation is the ~25 % reduction in the size of cells. The reduced size of starved cells would be expected due to growth factor-responsive restriction point control of the cell cycle which blocks progression early in G1 and causes exit from the cycle prior to completing G1 and G2 growth phases [14,31,44]. Mitogenic factor withdrawal also induces autophagy which could further contribute to reducing cell size [25]. Smaller size reduces the surface-to-volume ratio and intracellular water concentration, which is expected to enhance exchange of water and cryoprotectant [60]. Additionally, the small size after thawing could lead to better localization to targeted tissues. It has been frequently observed in animal models that the vast bulk of intravenously administered MSC trap in the lungs and are quickly cleared by lung resident macrophages [12,18,19,45,51]. The smaller cell size of G0/G1 synchronized cells could promote transit of lung microvasculature; thereby enhancing the probability that systemically delivered MSC will reach the injured or diseased target tissues [18,19,45,51].

In summary, we describe here a simple GMP-compliant manufacturing step for enhancing post-thaw recovery of cryopreserved MSC. This process should remove barriers to clinical development and ultimately post-approval marketing caused by the logistical challenges due to poor effectiveness of cryopreserved cells. Furthermore, the higher activity, combined with smaller size, is likely to enhance the pharmacokinetic and pharmacodynamic properties of thawed MSC, which should, in turn, increase effectiveness over normally cultured and cryopreserved cells [49]. Assuming greater potency is observed in clinical studies, the cost per dose of starved cells should be significantly lower than that for non-starved cells.

Funding sources

Research reported in this publication was supported by the National Institute of Allergy and Ifectious Disease of the National Institutes of Health under award number 5U01AI138334.

Declarations

Brian H. Johnstone, Dongsheng Gu, Chieh-Han Lin, Jianguang Du, and Erik J. Woods are current or former employees of Ossium Health, Inc., and have equity and/or options to purchase equity in Ossium Health, Inc.

Acknowledgements

We thank the Karen Pollok Laboratory at Indiana University for assistance with immunofluorescence microscopy.

Appendix A. Supplementary data

Supplementary data to this article can be found online at https://doi.org/10.1016/j.cryobiol.2023.104592.

References

[1] A. Abazari, B.J. Hawkins, A.J. Mathew, The impact of feeding regimen and cell cycle on post-thaw recovery in a human T-cell mode, Cytotherapy 21 (5) (2019) 116, https://doi.org/10.1016/j.jcyt.2019.03.384.

[2] J.P. Acker, M. Bondarovych, R. Brunotte, I.A. Buriak, B.J. Fuller, B. Glasmacher, A. M. Golsev, J. Gregor, O. Gryshkov, K. Herrity, B. Honegrova, C.J. Hunt, M. Jandova, B.H. Johnstone, P. Kilbride, M. Lanska, J. Mann, P. Mericka, K. B. Musal, V. Mutsenko, O. Mykhailova, Y. Petrenko, J. Radocha, A.M. Sherry, G. N. Stacey, L. Sterba, D. Vokurkova, N. William, E.J. Woods, Preservation and storage of cells for therapy: current applications and protocols, in: J.M. Gimble, D. Marolt Presen, R.O.C. Oreffo, S. Wolbank, H. Redl (Eds.), Cell Engineering and Regeneration. Reference Series in Biomedical Engineering, Springer, Cham, 2022, pp. 27–30, https://doi.org/10.1007/978-3-319-37076-7_68-2.

[3] L.L. Alekseenko, M.A. Shilina, O.G. Lyublinskaya, J.S. Kornienko, O.V. Anatskaya, A.E. Vinogradov, T.M. Grinchuk, I.I. Fridlyanskaya, N.N. Nikolsky, Quiescent human mesenchymal stem cells are more resistant to heat stress than cycling cells, Stem Cell. Int. (2018), 3753547, https://doi.org/10.1155/2018/3753547, 2018.

[4] S. Bahsoun, K. Coopman, E.C. Akam, Quantitative assessment of the impact of cryopreservation on human bone marrow-derived mesenchymal stem cells: up to 24 h post-thaw and beyond, Stem Cell Res. Ther. 11 (1) (2020, Dec 14) 540, https://doi.org/10.1186/s13287-020-02054-2.

[5] J.M. Baust, K.K. Snyder, R.G. Van Buskirk, J.G. Baust, Assessment of the impact of post-thaw stress pathway modulation on cell recovery following cryopreservation in a hematopoietic progenitor cell model, Cells 11 (2) (2022, Jan 14), https://doi.org/10.3390/cells11020278.

[6] A.K. Bryan, V.C. Hecht, W. Shen, K. Payer, W.H. Grover, S.R. Manalis, Measuring single cell mass, volume, and density with dual suspended microchannel resonators, Lab Chip 14 (3) (2014, Feb 7) 569–576, https://doi.org/10.1039/c3lc51022k.

[7] C. Cadart, S. Monnier, J. Grilli, P.J. Saez, N. Srivastava, R. Attia, E. Terriac, B. Baum, M. Cosentino-Lagomarsino, M. Piel, Size control in mammalian cells involves modulation of both growth rate and cell cycle duration, Nat. Commun. 9 (1) (2018, Aug 16) 3275, https://doi.org/10.1038/s41467-018-05393-0.

[8] C. Cadart, L. Venkova, M. Piel, M. Cosentino Lagomarsino, Volume growth in animal cells is cell cycle dependent and shows additive fluctuations, Elife 11 (2022, Jan 28), https://doi.org/10.7554/eLife.70816.

[9] H.X. Chao, C.E. Poovey, A.A. Privette, G.D. Grant, H.Y. Chao, J.G. Cook, J. E. Purvis, Orchestration of DNA damage checkpoint dynamics across the human cell cycle, Cell Syst 5 (5) (2017, Nov 22) 445–459 e445, https://doi.org/10.1016/j.cels.2017.09.015.

[10] R. Chinnadurai, I.B. Copland, M.A. Garcia, C.T. Petersen, C.N. Lewis, E.K. Waller, A.D. Kirk, J. Galipeau, Cryopreserved mesenchymal stromal cells are susceptible to T-cell mediated apoptosis which is partly rescued by IFNgamma licensing, Stem Cell. 34 (9) (2016, Sep) 2429–2442, https://doi.org/10.1002/stem.2415.

[11] R. Contreras-Lopez, R. Elizondo-Vega, M.J. Paredes, N. Luque-Campos, M. J. Torres, G. Tejedor, A.M. Vega-Letter, A. Figueroa-Valdes, C. Pradenas, K. Oyarce, C. Jorgensen, M. Khoury, M.L.A. Garcia-Robles, C. Altamirano, F. Djouad, P. Luz-Crawford, HIF1alpha-dependent metabolic reprogramming governs mesenchymal stem/stromal cell immunoregulatory functions, Faseb. J. 34 (6) (2020, Jun) 8250–8264, https://doi.org/10.1096/fj.201902232R.

[12] E. Eggenhofer, V. Benseler, A. Kroemer, F.C. Popp, E.K. Geissler, H.J. Schlitt, C. C. Baan, M.H. Dahlke, M.J. Hoogduijn, Mesenchymal stem cells are short-lived and do not migrate beyond the lungs after intravenous infusion, Front. Immunol. 3 (2012) 297, https://doi.org/10.3389/fimmu.2012.00297.

[13] M. Falk, I. Falkova, O. Kopecna, A. Bacikova, E. Pagacova, D. Simek, M. Golan, S. Kozubek, M. Pekarova, S.E. Follett, B. Klejdus, K.W. Elliott, K. Varga, O. Tepla, I. Kratochvilova, Chromatin architecture changes and DNA replication fork collapse are critical features in cryopreserved cells that are differentially controlled by cryoprotectants, Sci. Rep. 8 (1) (2018, Oct 2), 14694, https://doi.org/10.1038/s41598-018-32939-5.

[14] D.A. Foster, P. Yellen, L. Xu, M. Saqcena, Regulation of G1 cell cycle progression: distinguishing the restriction point from a nutrient-sensing cell growth checkpoint (s), Genes Cancer 1 (11) (2010, Nov) 1124–1131, https://doi.org/10.1177/1947601910392989.

[15] M. Francois, I.B. Copland, S. Yuan, R. Romieu-Mourez, E.K. Waller, J. Galipeau, Cryopreserved mesenchymal stromal cells display impaired immunosuppressive properties as a result of heat-shock response and impaired interferon-gamma licensing, Cytotherapy 14 (2) (2012, Feb) 147–152, https://doi.org/10.3109/14653249.2011.623691.

[16] J. Galipeau, The mesenchymal stromal cells dilemma–does a negative phase III trial of random donor mesenchymal stromal cells in steroid-resistant graft-versus-host disease represent a death knell or a bump in the road? Cytotherapy 15 (1) (2013, Jan) 2–8, https://doi.org/10.1016/j.jcyt.2012.10.002.

[17] J. Galipeau, L. Sensebe, Mesenchymal stromal cells: clinical challenges and therapeutic opportunities, Cell Stem Cell 22 (6) (2018, Jun 1) 824–833, https://doi.org/10.1016/j.stem.2018.05.004.

[18] J. Gao, J.E. Dennis, R.F. Muzic, M. Lundberg, A.I. Caplan, The dynamic in vivo distribution of bone marrow-derived mesenchymal stem cells after infusion, Cells Tissues Organs 169 (1) (2001) 12–20, https://doi.org/10.1159/000047856.

[19] J. Ge, L. Guo, S. Wang, Y. Zhang, T. Cai, R.C. Zhao, Y. Wu, The size of mesenchymal stem cells is a significant cause of vascular obstructions and stroke, Stem Cell Rev Rep 10 (2) (2014, Apr) 295–303, https://doi.org/10.1007/s12015-013-9492-x.

[20] J.V. Harper, G. Brooks, The mammalian cell cycle: an overview, Methods Mol. Biol. 296 (2005) 113–153, https://doi.org/10.1385/1-59259-857-9:113.

[21] T.T. Ho, M.R. Warr, E.R. Adelman, O.M. Lansinger, J. Flach, E.V. Verovskaya, M. E. Figueroa, E. Passegue, Autophagy maintains the metabolism and function of young and old stem cells, Nature 543 (7644) (2017, Mar 9) 205–210, https://doi.org/10.1038/nature21388.

[22] B.H. Johnstone, H.M. Miller, M.R. Beck, D. Gu, S. Thirumala, M. LaFontaine, G. Brandacher, E.J. Woods, Identification and characterization of a large source of primary mesenchymal stem cells tightly adhered to bone surfaces of human vertebral body marrow cavities, Cytotherapy 22 (11) (2020, Nov) 617–628, https://doi.org/10.1016/j.jcyt.2020.07.003.

[23] R.L. Kadle, S.A. Abdou, A.P. Villarreal-Ponce, M.A. Soares, D.L. Sultan, J.A. David, J. Massie, W.J. Rifkin, P. Rabbani, D.J. Ceradini, Microenvironmental cues enhance mesenchymal stem cell-mediated immunomodulation and regulatory T-cell expansion, PLoS One 13 (3) (2018), e0193178, https://doi.org/10.1371/journal.pone.0193178.

[24] K. Keren, P.T. Yam, A. Kinkhabwala, A. Mogilner, J.A. Theriot, Intracellular fluid flow in rapidly moving cells, Nat. Cell Biol. 11 (10) (2009, Oct) 1219–1224, https://doi.org/10.1038/ncb1965.

[25] B. Li, C. Sun, J. Sun, M.H. Yang, R. Zuo, C. Liu, W.R. Lan, M.H. Liu, B. Huang, Y. Zhou, Autophagy mediates serum starvation-induced quiescence in nucleus pulposus stem cells by the regulation of P27, Stem Cell Res. Ther. 10 (1) (2019, Apr 15) 118, https://doi.org/10.1186/s13287-019-1219-8.

[26] Z.H. Li, Y.L. Wang, H.J. Wang, J.H. Wu, Y.Z. Tan, Rapamycin-preactivated autophagy enhances survival and differentiation of mesenchymal stem cells after transplantation into infarcted myocardium, Stem Cell Rev Rep 16 (2) (2020, Apr) 344–356, https://doi.org/10.1007/s12015-020-09952-1.

[27] R. Liang, T. Arif, S. Kalmykova, A. Kasianov, M. Lin, V. Menon, J. Qiu, J.M. Bernitz, K. Moore, F. Lin, D.L. Benson, N. Tzavaras, M. Mahajan, D. Papatsenko, S. Ghaffari, Restraining lysosomal activity preserves hematopoietic stem cell quiescence and potency, Cell Stem Cell 26 (3) (2020, Mar 5) 359–376 e357, https://doi.org/10.1016/j.stem.2020.01.013.

[28] Y. Liu, X. Yuan, N. Munoz, T.M. Logan, T. Ma, Commitment to aerobic glycolysis sustains immunosuppression of human mesenchymal stem cells, Stem Cells Transl Med 8 (1) (2019, Jan) 93–106, https://doi.org/10.1002/sctm.18-0070.

[29] L.J. Mah, A. El-Osta, T.C. Karagiannis, gammaH2AX: a sensitive molecular marker of DNA damage and repair, Leukemia 24 (4) (2010, Apr) 679–686, https://doi.org/10.1038/leu.2010.6.

[30] O. Marescal, I.M. Cheeseman, Cellular mechanisms and regulation of quiescence, Dev. Cell 55 (3) (2020, Nov 9) 259–271, https://doi.org/10.1016/j.devcel.2020.09.029.

[31] S. Marguerat, A. Schmidt, S. Codlin, W. Chen, R. Aebersold, J. Bahler, Quantitative analysis of fission yeast transcriptomes and proteomes in proliferating and quiescent cells, Cell 151 (3) (2012, Oct 26) 671–683, https://doi.org/10.1016/j.cell.2012.09.019.

[32] M.A. Matthay, C.S. Calfee, H. Zhuo, B.T. Thompson, J.G. Wilson, J.E. Levitt, A. J. Rogers, J.E. Gotts, J.P. Wiener-Kronish, E.K. Bajwa, M.P. Donahoe, B.J. McVerry, L.A. Ortiz, M. Exline, J.W. Christman, J. Abbott, K.L. Delucchi, L. Caballero, M. McMillan, D.H. McKenna, K.D. Liu, Treatment with allogeneic mesenchymal stromal cells for moderate to severe acute respiratory distress syndrome (START study): a randomised phase 2a safety trial, Lancet Respir. Med. 7 (2) (2019, Feb) 154–162, https://doi.org/10.1016/S2213-2600(18)30418-1.

[33] I. McClain-Caldwell, L. Vitale-Cross, B. Mayer, M. Krepuska, M. Boyajian, V. Myneni, D. Martin, , Genomics, Computational Biology, C, K. Marko, K. Nemeth, E. Mezey, Immunogenic potential of human bone marrow mesenchymal stromal cells is enhanced by hyperthermia, Cytotherapy 20 (12) (2018, Dec) 1437–1444, https://doi.org/10.1016/j.jcyt.2018.10.002.

[34] L.E. McGann, H.E. Frey, Effect of hypertonicity and freezing on survival of unprotected synchronized mammalian cells, Cryobiology 9 (2) (1972, Apr) 107–111, https://doi.org/10.1016/0011-2240(72)90017-x.

[35] L.E. McGann, J. Kruuv, Freeze-Thaw damage in protected and unprotected synchronized mammalian cells, Cryobiology 14 (4) (1977, Aug) 503–505, https://doi.org/10.1016/0011-2240(77)90014-1.

[36] M. Mendicino, A.M. Bailey, K. Wonnacott, R.K. Puri, S.R. Bauer, MSC-based product characterization for clinical trials: an FDA perspective, Cell Stem Cell 14 (2) (2014, Feb 6) 141–145, https://doi.org/10.1016/j.stem.2014.01.013.

[37] J. Meneghel, P. Kilbride, G.J. Morris, Cryopreservation as a key element in the successful delivery of cell-based therapies-A review, Front. Med. 7 (2020), 592242, https://doi.org/10.3389/fmed.2020.592242.

[38] E. Moeendarbary, L. Valon, M. Fritzsche, A.R. Harris, D.A. Moulding, A. J. Thrasher, E. Stride, L. Mahadevan, G.T. Charras, The cytoplasm of living cells behaves as a poroelastic material, Nat. Mater. 12 (3) (2013, Mar) 253–261, https://doi.org/10.1038/nmat3517.

[39] G. Moll, J.J. Alm, L.C. Davies, L. von Bahr, N. Heldring, L. Stenbeck-Funke, O. A. Hamad, R. Hinsch, L. Ignatowicz, M. Locke, H. Lonnies, J.D. Lambris, Y. Teramura, K. Nilsson-Ekdahl, B. Nilsson, K. Le Blanc, Do cryopreserved mesenchymal stromal cells display impaired immunomodulatory and therapeutic properties? Stem Cell. 32 (9) (2014, Sep) 2430–2442, https://doi.org/10.1002/stem.1729.

[40] W.C. Mu, R. Ohkubo, A. Widjaja, D. Chen, The mitochondrial metabolic checkpoint in stem cell aging and rejuvenation, Mech. Ageing Dev. 188 (2020, Jun), 111254, https://doi.org/10.1016/j.mad.2020.111254.

[41] A. Muslimovic, I.H. Ismail, Y. Gao, O. Hammarsten, An optimized method for measurement of gamma-H2AX in blood mononuclear and cultured cells, Nat. Protoc. 3 (7) (2008) 1187–1193, https://doi.org/10.1038/nprot.2008.93.

[42] L. Olmedo-Moreno, Y. Aguilera, C. Balina-Sanchez, A. Martin-Montalvo, V. Capilla-Gonzalez, Heterogeneity of in vitro expanded mesenchymal stromal cells and strategies to improve their therapeutic actions, Pharmaceutics 14 (5) (2022, May 23), https://doi.org/10.3390/pharmaceutics14051112.

[43] O. Padovan-Merhar, G.P. Nair, A.G. Biaesch, A. Mayer, S. Scarfone, S.W. Foley, A. R. Wu, L.S. Churchman, A. Singh, A. Raj, Single mammalian cells compensate for differences in cellular volume and DNA copy number through independent global transcriptional mechanisms, Mol. Cell 58 (2) (2015, Apr 16) 339–352, https://doi.org/10.1016/j.molcel.2015.03.005.

[44] A.B. Pardee, A restriction point for control of normal animal cell proliferation, Proc. Natl. Acad. Sci. U. S. A 71 (4) (1974, Apr) 1286–1290, https://doi.org/10.1073/pnas.71.4.1286.

[45] R.F. Pereira, K.W. Halford, M.D. O'Hara, D.B. Leeper, B.P. Sokolov, M.D. Pollard, O. Bagasra, D.J. Prockop, Cultured adherent cells from marrow can serve as long-lasting precursor cells for bone, cartilage, and lung in irradiated mice, Proc. Natl. Acad. Sci. U. S. A 92 (11) (1995, May 23) 4857–4861, https://doi.org/10.1073/pnas.92.11.4857.

[46] G. Pontarin, P. Ferraro, C. Rampazzo, G. Kollberg, E. Holme, P. Reichard, V. Bianchi, Deoxyribonucleotide metabolism in cycling and resting human fibroblasts with a missense mutation in p53R2, a subunit of ribonucleotide reductase, J. Biol. Chem. 286 (13) (2011, Apr 1) 11132–11140, https://doi.org/10.1074/jbc.M110.202283.

[47] J.T. Rodgers, K.Y. King, J.O. Brett, M.J. Cromie, G.W. Charville, K.K. Maguire, C. Brunson, N. Mastey, L. Liu, C.R. Tsai, M.A. Goodell, T.A. Rando, mTORC1 controls the adaptive transition of quiescent stem cells from G0 to G(Alert), Nature 510 (7505) (2014, Jun 19) 393–396, https://doi.org/10.1038/nature13255.

[48] E.P. Rogakou, D.R. Pilch, A.H. Orr, V.S. Ivanova, W.M. Bonner, DNA double-stranded breaks induce histone H2AX phosphorylation on serine 139, J. Biol. Chem. 273 (10) (1998, Mar 6) 5858–5868, https://doi.org/10.1074/jbc.273.10.5858.

[49] M. Salvadori, N. Cesari, A. Murgia, P. Puccini, B. Riccardi, M. Dominici, Dissecting the pharmacodynamics and pharmacokinetics of MSCs to overcome limitations in their clinical translation, Mol Ther Methods Clin Dev 14 (2019, Sep 13) 1–15, https://doi.org/10.1016/j.omtm.2019.05.004.

[50] K.L. Santucci, J.M. Baust, K.K. Snyder, R.G. Van Buskirk, J.G. Baust, Investigation of the impact of cell cycle stage on freeze response sensitivity of androgen-insensitive prostate cancer, Technol. Cancer Res. Treat. 15 (4) (2016, Aug) 609–617, https://doi.org/10.1177/1533034616648059.

[51] S. Schrepfer, T. Deuse, H. Reichenspurner, M.P. Fischbein, R.C. Robbins, M. P. Pelletier, Stem cell transplantation: the lung barrier, Transplant. Proc. 39 (2) (2007, Mar) 573–576, https://doi.org/10.1016/j.transproceed.2006.12.019.

[52] S. Son, J.H. Kang, S. Oh, M.W. Kirschner, T.J. Mitchison, S. Manalis, Resonant microchannel volume and mass measurements show that suspended cells swell during mitosis, J. Cell Biol. 211 (4) (2015, Nov 23) 757–763, https://doi.org/10.1083/jcb.201505058.

[53] S. Subramaniam, P. Sreenivas, S. Cheedipudi, V.R. Reddy, L.S. Shashidhara, R. K. Chilukoti, M. Mylavarapu, J. Dhawan, Distinct transcriptional networks in quiescent myoblasts: a role for Wnt signaling in reversible vs. irreversible arrest, PLoS One 8 (6) (2014), e65097, https://doi.org/10.1371/journal.pone.0065097.

[54] A. Tzur, R. Kafri, V.S. LeBleu, G. Lahav, M.W. Kirschner, Cell growth and size homeostasis in proliferating animal cells, Science 325 (5937) (2009, Jul 10) 167–171, https://doi.org/10.1126/science.1174294.

[55] J.R. Valcourt, J.M. Lemons, E.M. Haley, M. Kojima, O.O. Demuren, H.A. Coller, Staying alive: metabolic adaptations to quiescence, Cell Cycle 11 (9) (2012, May 1) 1680–1696, https://doi.org/10.4161/cc.19879.

[56] C. Van Rechem, G. Boulay, S. Pinte, N. Stankovic-Valentin, C. Guerardel, D. Leprince, Differential regulation of HIC1 target genes by CtBP and NuRD, via an acetylation/SUMOylation switch, in quiescent versus proliferating cells, Mol. Cell Biol. 30 (16) (2010, Aug) 4045–4059, https://doi.org/10.1128/MCB.00582-09.

[57] C.T.J. van Velthoven, T.A. Rando, Stem cell quiescence: dynamism, restraint, and cellular idling, Cell Stem Cell 24 (2) (2019, Feb 7) 213–225, https://doi.org/10.1016/j.stem.2019.01.001.

[58] Z. Wang, Regulation of cell cycle progression by growth factor-induced cell signaling, Cells 10 (12) (2021, Nov 26), https://doi.org/10.3390/cells10123327.

[59] R.M. Wise, S. Al-Ghadban, M.A.A. Harrison, B.N. Sullivan, E.R. Monaco, S. J. Aleman, U.M. Donato, B.A. Bunnell, Short-term autophagy preconditioning upregulates the expression of COX2 and PGE2 and alters the immune phenotype of human adipose-derived stem cells in vitro, Cells 11 (9) (2022, Apr 19), https://doi.org/10.3390/cells11091376.

[60] E.J. Woods, S. Thirumala, S.S. Badhe-Buchanan, D. Clarke, A.J. Mathew, Off the shelf cellular therapeutics: factors to consider during cryopreservation and storage of human cells for clinical use, Cytotherapy 18 (6) (2016, Jun) 697–711, https://doi.org/10.1016/j.jcyt.2016.03.295.

[61] S. Zhang, X. Zhang, K. Wang, X. Xu, M. Li, J. Zhang, Y. Zhang, J. Hao, X. Sun, Y. Chen, X. Liu, Y. Chang, R. Jin, H. Wu, Q. Ge, Newly generated CD4(+) T cells acquire metabolic quiescence after thymic egress, J. Immunol. 200 (3) (2018, Feb 1) 1064–1077, https://doi.org/10.4049/jimmunol.1700721.

[62] K. Zielniok, A. Burdzinska, B. Kaleta, R. Zagozdzon, L. Paczek, Vadadustat, a HIF prolyl hydroxylase inhibitor, improves immunomodulatory properties of human mesenchymal stromal cells, Cells 9 (11) (2020, Nov 1), https://doi.org/10.3390/cells9112396.

[63] E. Zlotek-Zlotkiewicz, S. Monnier, G. Cappello, M. Le Berre, M. Piel, Optical volume and mass measurements show that mammalian cells swell during mitosis, J. Cell Biol. 211 (4) (2015, Nov 23) 765–774, https://doi.org/10.1083/jcb.201505056.